IOP PUBLISHING NANOTECHNOLOGY
Nanotechnology **18** (2007) 175101 (9pp) doi:10.1088/0957-4484/18/17/175101

Magnetic nanoparticles as bimodal tools in magnetically induced labelling and magnetic heating of tumour cells: an *in vitro* study

M Kettering[1,7], J Winter[1], M Zeisberger[2], S Bremer-Streck[3], H Oehring[4], C Bergemann[5], C Alexiou[6], R Hergt[2], K J Halbhuber[4], W A Kaiser[1] and I Hilger[1,7]

[1] Institute of Diagnostic and Interventional Radiology, University Hospital Jena, Erlanger Allee 101, D-07747 Jena, Germany
[2] Institute for Physical High Technology, Postfach 100 239, D-07702 Jena, Germany
[3] Institute of Clinical Chemistry and Laboratory Medicine, University Hospital Jena, Bachstraße 18, D-07740 Jena, Germany
[4] Institute of Anatomy II, University Hospital Jena, Teichgraben 7, D-07743 Jena, Germany
[5] Chemicell GmbH, Wartburgstraße 6, D-10823 Berlin, Germany
[6] Department of Otorhinolaryngology, Head and Neck Surgery, University Erlangen-Nürnberg, Waldstraße 1, D-91054 Erlangen, Germany

E-mail: melanie.kettering@med.uni-jena.de and ingrid.hilger@med.uni-jena.de

Received 3 November 2006, in final form 29 December 2006
Published 2 April 2007
Online at stacks.iop.org/Nano/18/175101

Abstract
Localized magnetic heating treatments (hyperthermia, thermal ablation) using superparamagnetic iron oxide nanoparticles continue to be an active area of cancer research. The present study uses magnetic nanoparticles (MNP) as bimodal tools and combines magnetically induced cell labelling and magnetic heating. The main focus was to assess if a selective and higher MNP accumulation within tumour cells due to magnetic labelling (max. 56 and 83 mT) and consequently a larger heating effect occurs after exposure to an alternating magnetic field (magnetic heating: frequency 400 kHz, amplitude 24.6 kA m^{-1}) in order to eliminate labelled tumour cells effectively. The results demonstrate that the magnetically based cellular MNP uptake by human adenocarcinoma cells is due to suitable magnetic field gradients *in vitro* which intensify the temperature increase generated during magnetic heating. A significantly ($P \leqslant 0.05$) enhanced MNP cell uptake due to 83 mT labelling compared to controls or to 56 mT labelling was observed. Our experiments required the following conditions, namely a cell concentration of 2.5×10^7 cells ml^{-1}, a minimum MNP concentration of 0.32 mg Fe ml^{-1} culture medium, and an incubation time of 24 h, to reach this effect as well as for the significantly enlarged heating effects to occur.

1. Introduction

The uncontrolled growth and spread of malignant cells that can affect almost any tissue of the body remain a major burden to human health. During the past decades, thermal treatment modalities have become an area of considerable interest in cancer therapy. Thermal energy producing temperatures between 40 and 44 °C deactivate normal cellular processes in a dose-dependent manner (hyperthermia, e.g. [1, 2]). Cells or tissues exposed to temperatures above this level show

[7] Authors to whom any correspondence should be addressed.

 © 2007 IOP Publishing Ltd Printed in the UK

areas of extensive necrosis known as thermal ablation [3]. Since thermal therapies have become promising approaches for cancer treatment, one of the most important issues is how to target the heat appropriately. Thereby, magnetic nanoparticles (MNP) seem to be suitable tools for heat targeting.

Based on their physical, chemical, thermal and mechanical properties, MNP offer—beside hyperthermal or thermal ablative therapies—a high potential for several biomedical applications, such as cellular therapy, tissue repair, drug delivery, magnetic resonance imaging (MRI), hyperthermia or magnetofection [4]. For these purposes, MNP have to be biocompatible and have to have interactive functional groups at their surface for further functionalization with bioactive molecules [5]. In contrast to SPIOs (superparamagnetic iron oxide particles) or USPIOs (ultrasmall superparamagnetic iron oxide particles) used for MRI [6] which have very small particle core diameters ($\leqslant$6 nm) and though are not able to generate heating effects [7], superparamagnetic iron oxide particles for heating modalities have to be larger in size ($\geqslant$10 nm) to reach cytotoxic effects within target cells [7].

For reaching cytotoxic effects in tumour tissues, MNP have to be deposited there and exposed to an alternating magnetic field which generates heat as a result of losses due to hysteresis, Néel or Brown relaxation [8]. Although the use of MNP for thermal therapies was proposed nearly 50 years ago [9], in the last decade, progress has been made particularly with MNP composed of iron oxides, such as magnetite and maghemite [4, 10] as potential tools for cancer treatment by means of magnetic heating (e.g. [4, 10–13]). Preclinical investigations with tumour cells *in vitro* [14] and intra-tumoural injections of MNP in mice [14, 15] have shown that, when a temperature of 55–60 °C was reached (magnetic thermal ablation), complete cell death occurred in treated cells or tissues within a few minutes.

Furthermore, to selectively destroy multi-focal tumours, MNP coupled with tumour-specific antibodies were injected into the vascular system *in vivo*, allowing the affected regions to be targeted [16]. Yet in contrast to intra-tumoural application, comparatively lower amounts of magnetic material may be expected to accumulate within the tumour region due to its large deposition, for example, in the liver [16]. Thus, during magnetic heating, smaller temperature increases (hyperthermic temperatures) could be observed, leading to only 50% tumour regression [17]. Therefore, other therapy modalities should be combined with magnetic heating procedures to increase the therapeutic effect. Interesting studies have shown that MNP can be used as tools to transport bound chemotherapeutics to tumour loci *in vivo* [18–21]. In this context, intra-arterially injected MNP labelled with chemotherapeutics in rabbits were concentrated specifically in the desired area using an external magnetic field (magnetic drug targeting) [22]. This method was also used successfully in patients [23].

The purpose of our study was to assess the combination effects of magnetically induced cell labelling (permanent magnet) with magnetic heating (alternating magnetic field) for the first time. The combination was achieved by using a common tool (MNP) for both therapeutic modalities. Using human adenocarcinoma cells *in vitro*, we wanted to determine (1) whether increased MNP accumulation in tumour cells by means of magnetic gradient fields is possible; and (2) whether this particle accumulation is related to an enhanced heating effect in a magnetic alternating field.

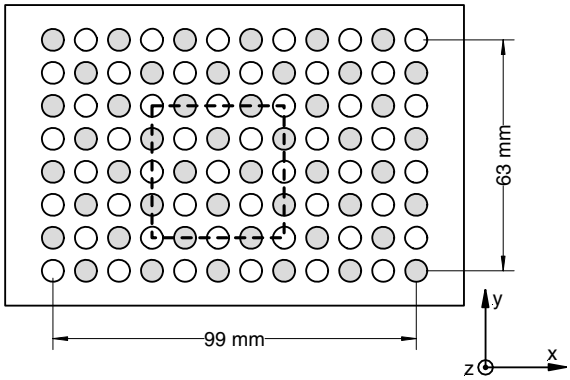

Figure 1. Array of 12 × 8 permanent magnets (top view). The grey or white circles indicate the orientation of the magnets with the north pole or the south pole on top, respectively. The dashed square represents the area where the field distribution was measured.

2. Experimental section

2.1. Magnetic material

An aqueous colloidal suspension of biocompatible, superparamagnetic, starch-coated iron oxide MNP (fluidMAG-D: chemicell GmbH, Berlin, Germany) was used for the experiments. MNP were suspended in bidistilled water, autoclaved and aggregation-stabilized under various physiological conditions (http://www.chemicell.com/home/index.html). The magnetite core size was determined by a vibrating sample magnetometer (VSM) using the method proposed by Chantrell *et al* [24]. The mean value of the hydrodynamic diameter of the MNP was measured at 25 °C, using a Zetasizer Nano ZS (Malvern, Herrenberg, Germany).

The morphology of MNP was assessed by transmission electron microscopy (TEM) (Zeiss EM 902A). A sample of starch coated MNP was diluted to 0.01% solid content with distilled water. 10 μl of this sample was placed on a formvar coated copper grid. The samples were dried at 20 °C and observed with an accelerating voltage of 80 kV. Additional contrasting was not applied.

2.2. Magnet plates

Two arrays of permanent magnets (magnet A and magnet B) with different field strengths but the same geometry were used. Each array consisted of 12 × 8 cylindric NdFeB magnets of 4.5 mm diameter arranged with alternating polarity (figure 1). In order to characterize these arrays, the distribution of the vertical component of the magnetic induction (B_z) was scanned within an area of Δx x $\Delta y = 36 \times 36$ mm^2 (dashed square in figure 1) at different distances in the z direction above the surface (2.2 and 4 mm, respectively). This was also done to describe the magnetic field strength acting on the cell layer (2.2 mm). Due to the periodicity of the arrangement, only a representative part of the magnet surface was scanned. Scanning was performed using a Hall probe attached to a three-axis positioning system.

2.3. Cell culture

The adherent invasive ductal breast carcinoma cell line BT-474 (American Tissue Culture Collection, Manassas, VA, USA, No. HTB-20) was cultured in Dulbecco's Modified Eagle Medium (DMEM, Gibco, Karlsruhe, Germany) containing 10% (v/v) foetal calf serum (FCS, Gibco, Karlsruhe, Germany) and 1% (v/v) 1 M HEPES (Gibco, Karlsruhe, Germany). Cells were incubated in a humidified incubator at 37 °C with 5% CO_2 and 95% relative humidity (HERAcell® CO_2-Inkubator, Kendro, Hanau, Germany) and were grown in culture flasks (growth area: 75 cm^2, maximal volume: 250 ml, volume of culture medium: 15 ml) until confluency was achieved.

2.4. Magnetic cell labelling

The MNP suspension was added to the confluent cell culture and the flasks were placed on magnet A or magnet B, respectively. Afterwards, cells were placed in a humidified incubator for defined time periods (see section 2.5). Cells without magnet arrays, with (control B) and without (control A) MNP incubation, served as controls for cellular MNP binding. After incubation, cells were washed with phosphate buffered saline (0.1 M PBS, pH 7.4) in order to remove unbound MNP. Next, cells were thoroughly harvested by a scrubber and counted with a Z2™ COULTER COUNTER® (Beckman Coulter GmbH, Krefeld, Germany). Then, cell concentrations were adjusted for heating experiments (see section 2.6).

2.5. Parameters for magnetic cell labelling

To verify if magnetic cell labelling of tumour cells with MNP and an external permanent magnet (magnetic cell labelling) is possible, the following experiments were performed:

To assess the heating effects on different cell numbers, cells were incubated with a defined MNP concentration (0.32 mg Fe ml^{-1}) over a period of time (24 h) in cell culture flasks. Then, different cell concentrations (0.5, 1, 2.5 and 5×10^7 BT-474 cells ml^{-1}, respectively) were exposed to an alternating magnetic field (magnetic heating, see section 2.6).

In the next step, different incubation times were used. BT-474 cells were incubated with MNP (0.32 mg Fe ml^{-1}) for 1, 3, 6, 12 and 24 h, respectively, and 2.5×10^7 BT-474 cells ml^{-1} were exposed to the alternating magnetic field.

Next the concentration of MNP was varied. Tumour cells were incubated with 0.16, 0.32 and 0.48 mg Fe, respectively, per ml culture medium for 24 h. Then 2.5×10^7 BT-474 cells ml^{-1} were exposed to the alternating magnetic field.

2.6. Magnetic heating of cells labelled with magnetic nanoparticles

The effect of MNP labelling of tumour cells on magnetically induced heating was assessed by exposing labelled or non-labelled cells to an alternating magnetic field (frequency 400 kHz, amplitude 24.6 kA m^{-1}) induced by a circular coil. Cell concentrations of 0.5, 1, 2.5 and 5×10^7 BT-474 cells per ml (total volume: 200 μl) were heated. The temperature increase was recorded by means of a thermocouple of copper and constantan wires (0.09 and 0.16 mm in diameter, respectively) connected to a multimeter with automatic registration (Keithley, Germering, Germany) as described previously [12]. In preliminary experiments, the results of heating the thermocouple in bidistilled water without iron oxide particles was found to be negligible. Experiments were performed 3–4 times. Temperature increases were measured over 327 s owing to technical reasons. At the beginning of the heating experiments, samples were determined to be at thermal equilibrium, with the initial temperatures of MNP suspensions kept within a range of 24 ± 2 °C.

Temperature increases (ΔT [K]) were calculated by

$$\Delta T = T_2 - T_1 \text{ [K]}$$

with T_1: first temperature value taken 4 s after powering on the alternating magnetic field (figure 4: $T_1 = 0$). T_2: last temperature value after switching off the alternating magnetic field.

The slope of the temperature curves (dT/dt [K s^{-1}]) was calculated by

$$\frac{dT}{dt} \approx \frac{T_2 - T_1}{t_2 - t_1} \text{ [K s}^{-1}\text{]}$$

with t_1: the point in time of the first temperature value above the initial temperature (figure 1: $T_1 = 0$), t_2: the point in time after switching off the alternating magnetic field.

2.7. Quantitative determination of iron contents of magnetically labelled cells

The iron contents of labelled cells and washing solutions were determined by flame atomic absorption spectrometry (AAS5 FL, Analytik Jena AG, Germany) with Acetylene-Air-Flame at the analytical line of 248.3 nm. 50 μl of the cell solutions were dissolved with 500 μl concentrated HCl and further diluted with deionized water (final dilutions; control A 1:6, control B 1:1386, 56 mT labelling 1:1386, 83 mT labelling 1:2640). Washing solutions were not diluted. Because of the high dilution ratio aqueous standard solutions can be used to calibrate iron (5, 10, 20, 30, 50 μmol l^{-1} Fe in 0.1 N HCl; Alfa Aesar Johnson Matthey GmbH, Karlsruhe, Germany).

2.8. Electron microscopy

BT-474 cells grown in DMEM (containing 10% (v/v) FCS and 1% (v/v) 1 M HEPES; Gibco, Karlsruhe, Germany) on 24 well plates up to a confluency of 90% were incubated with a defined MNP concentration (0.32 mg Fe ml^{-1}) in a humidified incubator at 37 °C over 24 h. Thereafter cell cultures were fixed with 2% (v/v) glutaraldehyde solution (0.1 M cacodylate buffer, pH 7.4) containing 5% sucrose at 20 °C for 30 min. In the next step the cell layers were washed in cacodylate buffer (0.1 M, pH 7.4, 6.8% sucrose) and postfixed with a freshly prepared mixture of 1 volume 2% OsO_4 (dissolved in distilled water) and 1 volume of 3% $K_4[Fe(CN)_6]$ in 0.2 M cacodylate buffer (pH 7.4) at 4 °C for 2 h [25]. After postfixation cells were rinsed with 0.1 M cacodylate buffer (pH 7.4, 6.8% sucrose) until the solution remained clear, dehydrated in graded series of ethanol and embedded in Epon 812 via hydroxypropylmethacrylate as intermedium. The cell sheets were finally cured in an oven at 60 °C for 6 days.

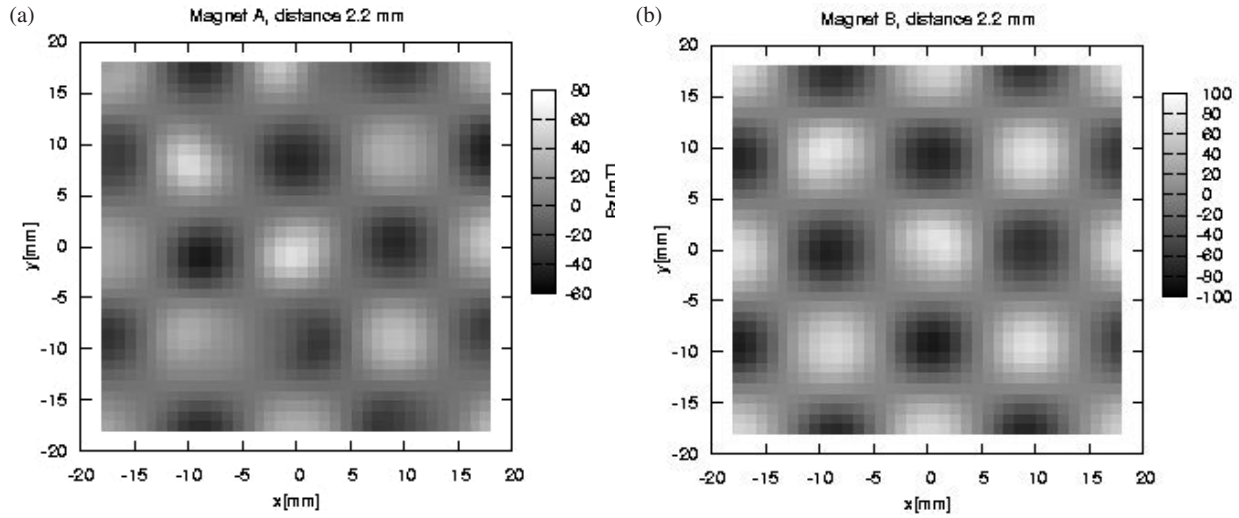

Figure 2. Field distribution $B_z(x, y)$ of magnet A (left) and magnet B (right) at $z = 2.2$ mm from the surface. The field was scanned within the selected area (see figure 1). Black and white scale [mT].

Utrathin sections were cut with a Leica Ultracut S ultramicrotome and stained as usual with uranyl acetate and lead citrate.

2.9. Statistical analysis

Mean values and standard deviations of the measured data were calculated. The differences of mean values among the experiments were investigated with the Student's t-test. Differences of $P \leqslant 0.05$ were considered to be statistically significant.

Calculated diameters of the magnetic cores of MNP as determined by TEM analysis were tested for normal distribution with the KOLMOGOROFF–SMIRNOFF one sample test. The significance level of $P < 0.01$ was used.

3. Results and discussion

3.1. Physicochemical characterization of the magnetic material

The magnetite core size of the superparamagnetic fluidMAG-D nanoparticles as determined from VSM data assuming a lognormal size distribution. We found a mean core diameter of $D = 11.4$ nm and a (lognormal) standard deviation $\sigma = 0.38$. The hydrodynamic diameter of the MNP measured with a Zetasizer Nano ZS was determined to be 217 nm.

Reaching an appropriate temperature increase that is able to damage cells *in vitro* and *in vivo* during magnetic heating with the alternating magnetic field parameters (frequency 400 kHz, amplitude 24.6 kA m^{-1}) used in previous investigations showed that the core size is decisive [26]. The core size of the contrast agent Endorem® (Guerbet S.A., Paris, France) was determined to be 3–5 nm and did not lead to suitable heating effects, whereas other MNP with a core size of 8–11 nm showed good heating properties in connection with the aforementioned parameters of the magnetic field [7].

3.2. Physical characterization of the magnet plates

The characterization of the field strength of the permanent magnets A and B using a Hall probe revealed an approximately periodical field distribution for the 2.2 mm space, which was the distance of the cell layer from the magnet (figure 2). When considering $y = 0$ (see figure 1), distinct field distributions of $B_z(x)$ were found (figure 3). The maximum values of $|B_z|$ were 56 mT for magnet A and 83 mT for magnet B at a distance of $z = 2.2$ mm from the surface of the magnets. At a distance of $z = 4$ mm, 21 mT for magnet A and 27 mT for magnet B were determined.

3.3. Magnetic heating and iron content of magnetically labelled cells

Generally, after magnetic labelling of cells with magnet B (83 mT), distinctly larger heating rates were found compared to magnet A (56 mT) and to cells labelled that lacked permanent magnets. Furthermore, magnetic labelling with magnet A did not lead to higher temperature increases compared to non-magnetically labelled cells.

Previous *in vitro* studies showed that the sedimentation of MNP depends on the applied magnetic field strength [27] and that an increased sedimentation of the MNP leads to a higher intracellular uptake caused by endocytosis [28]. These findings could explain the increased intracellular uptake of MNP using magnet B compared to the investigations using magnet A. Therefore, to achieve larger heating rates in tumours, it seems to be necessary to accumulate a high amount of MNP in the respective tissue. High enrichment of MNP can be carried out, for example, by active targeting using a strong magnetic field which is placed over the targeted area [29], by the use of MNP conjugated with tumour-specific antibodies [30] or direct intra-tumoural injection [14, 31].

A representative example of a higher temperature increase in dependence on the exposure time to an alternating magnetic field is shown in the particular case when cells were labelled with 0.32 mg Fe ml^{-1} culture medium for 24 h and 2.5 ×

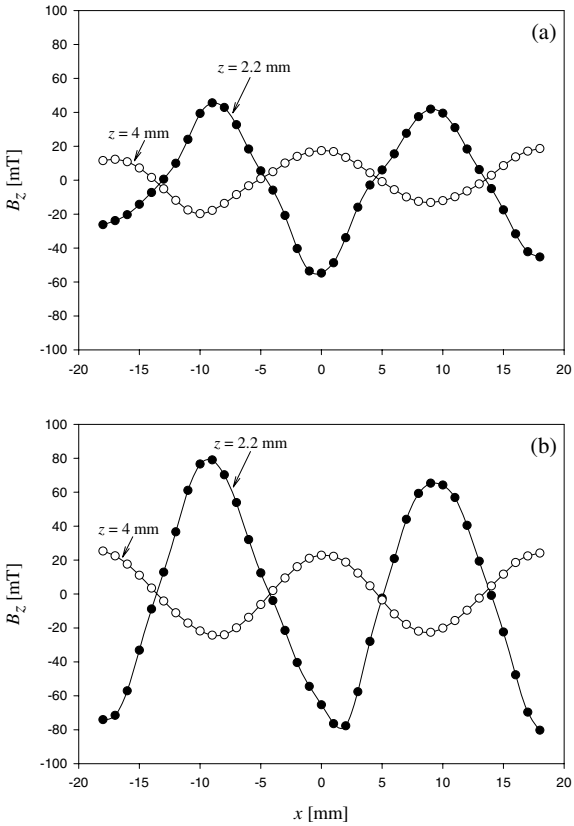

Figure 3. Field distribution $B_z(x)$ of magnet A (a) and magnet B (b) at $y = 0$ and $z = 2.2$ mm or 4.0 mm from the surface.

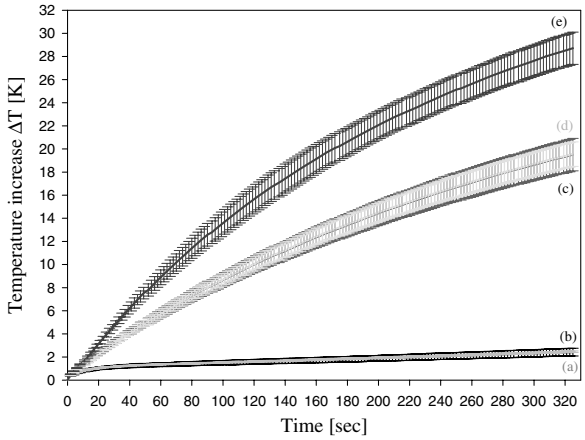

Figure 4. Temperature increase during the exposure of 5×10^6 BT-474 cells (200 μl of 2.5×10^7 BT-474 ml^{-1} cell suspension; confluent cells were incubated with 0.32 mg Fe ml^{-1} culture medium over 24 h) to an alternating magnetic field (frequency 400 kHz, amplitude 24.6 kA m^{-1}) for 327 s. (a) Bidistilled water, (b) cells without MNP and without magnetically induced labelling (control A), (c) cells containing MNP (100 ± 11 pg Fe/cell) without magnetically induced labelling (control B), (d) cells containing MNP (71 ± 4 pg Fe per cell) with 56 mT labelling (magnet A), (e) cells containing MNP (122 ± 7 pg Fe/cell) with 83 mT labelling (magnet B).

10^7 BT-474 cells ml^{-1} were subjected to magnetic heating (figure 4). BT-474 cells labelled by means of magnetic plates showed a significant ($P \leqslant 0.05$) temperature increase (treatment time: 5.45 min) of 28.2 ± 0.4 K when using magnet B (83 mT; slope dT/dt: 0.16 ± 0.02 K s^{-1}) and a temperature increase of 19.3 ± 0.8 K in connection with magnet plate A (56 mT; slope dT/dt: 0.098 ± 0.006 K s^{-1}), which is not different in comparison to cells incubated with MNP but lacking a magnet (temperature increase ΔT: 19.4 ± 1.4 K; slope dT/dt: 0.096 ± 0.007 K s^{-1}). For non-labelled cells and buffer alone, temperature increases of 2.5 ± 0.1 K (slope dT/dt: 0.013 ± 0.002 K s^{-1}) were measured. The latter observations may be related to the minor influence of induced eddy currents on the temperatures measured [32].

Obviously, MNP were bound tightly enough to cells and were incorporated into them, being able to withstand the washing procedure applied after the incubation. Moreover, an effect of unbound MNP on the reported temperature increases can be ruled out, because the iron contents of the last washing step were 1×10^6 times lower than those of the corresponding cell sample, showing that unbound MNP were sluiced out. Our data showed that the combination of magnetic labelling and magnetic heating led to a higher temperature increase in labelled cells compared to controls. The results also demonstrated that labelling cells with MNP may be improved by the application of suitable magnetic field gradients which attract the MNP toward the cells. Similarly, increased cell labelling was achieved using a magnetic field gradient, leading to an improved processing time in MNP-mediated gene transfer [33, 34].

In addition, the temperature rise of labelled and unlabelled BT-474 cells depended on cell concentration, incubation time, and MNP concentration and was related to their corresponding iron contents (see figures 5(a)–(f)). In the majority of cases, the observed temperature increases between the samples were reflected in the corresponding iron concentrations. With some exceptions, the effects associated with magnet B (83 mT) were significantly higher compared to magnet A (56 mT) or to samples treated with MNP without magnets (control B). Furthermore, the data showed that the magnetic induction of magnet A (56 mT) is not enough to enrich iron concentrations within tumour cells and, therefore, to obtain a higher temperature rise compared to tumour cells with MNP in the absence of magnets (control B).

With increasing cell concentrations in the sample, a steady temperature rise was observed (figure 5(a), III–V) compared to cells lacking MNP (figure 5(a) II). Heating of cells and the corresponding iron content per cell (figure 5(d)) treated with magnet B (83 mT) was in all cases significantly higher ($P \leqslant 0.05$) compared to samples treated with magnet A (56 mT) or samples without a magnet in the presence of MNP (control B).

The temperature rises (figure 5(b)) and iron concentrations (figure 5(e)) of labelled and unlabelled cells depending on the incubation time revealed a significant iron uptake of cells treated with magnet B (83 mT) compared to control B (cells with MNP, without a magnet) and magnet A (56 mT) and therefore a significant temperature increase only for the 24 h of incubation.

Increasing the MNP concentration in the culture medium from 0.16 to 0.48 mg Fe ml^{-1} resulted in a continuous increase of iron content (figure 5(f)) and of heat (figure 5(c)) for the

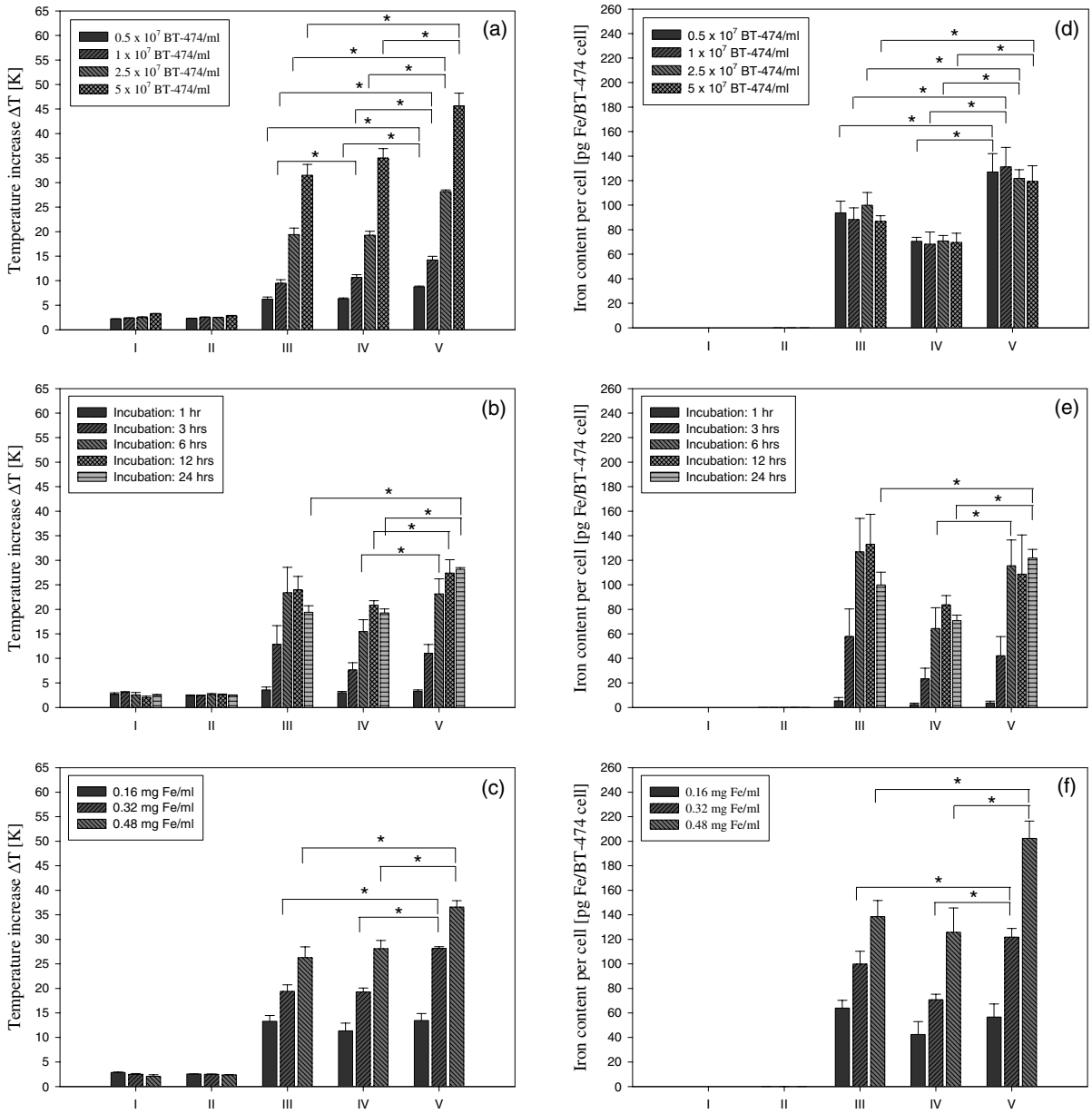

Figure 5. Temperature rise of labelled and non-labelled BT-474 cells depending on the (a) cell concentration exposed to an alternating magnetic field (0.32 mg Fe ml^{-1} culture medium; 24 h incubation of MNP), (b) incubation time of MNP (0.32 mg Fe ml^{-1} culture medium, 2.5×10^7 BT-474 cells ml^{-1} exposed to an alternating magnetic field) and (c) MNP concentration (24 h incubation of MNP, 2.5×10^7 BT-474 cells ml^{-1} exposed to an alternating magnetic field) and their corresponding iron contents ((d), (e), (f), respectively; [pg Fe/cell]); (I) bidistilled water, (II) cells without MNP, without magnet (control A), (III) cells with MNP, without magnet (control B), (IV) cells with MNP, with 56 mT labelling (magnet A), (V) cells with MNP, with 83 mT labelling (magnet B). * = values which were significantly ($P \leqslant 0.05$) different from control B or from 56 mT labelling.

single experimental approaches (III, IV and V, respectively). Incubating cells with 0.32 and 0.48 mg Fe ml^{-1} resulted in significantly higher iron concentrations and therefore significantly higher temperature increases in cells treated with magnet B (83 mT) compared to control B (cells with MNP, without magnet) and magnet A (56 mT).

To further analyse these findings, we correlated the temperature increases of labelled and unlabelled BT-474 cells with the iron content per cell as shown in figure 6 on the example of 0.32 mg Fe ml^{-1} culture medium incubated over 24 h and different cell concentrations in the alternating magnetic field. Our results demonstrated that a cell concentration of 2.5×10^7 cells ml^{-1} was necessary to significantly enlarge MNP cell uptake through magnetic labelling with magnet B (83 mT) compared to controls (figure 6, II and III) or to the 56 mT labelling of BT-474 cells.

The temperature elevations reported in the present study are based on measurements where sample set-ups *in vitro* were in a thermally highly insulated environment in comparison to the case of tumour cells in the *in vivo* situation. Taking into account that, among others, the effects of heat capacity, the conductivity of tissue and the temperature distribution

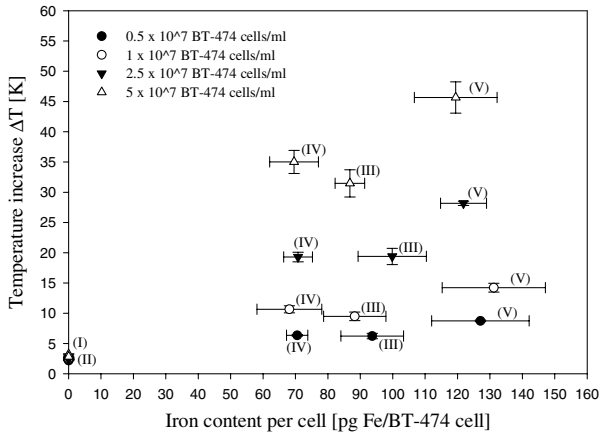

Figure 6. Correlation of temperature rises of labelled and non-labelled BT-474 cells with the corresponding iron contents (0.32 mg Fe ml^{-1} culture medium; 24 h incubation of MNP, variable cell concentrations exposed to an alternating magnetic field). (I) bidistilled water, (II) cells without MNP, without magnet (control A), (III) cells with MNP, without magnet (control B), (IV) cells with MNP, with 56 mT labelling (magnet A), (V) cells with MNP, with 83 mT labelling (magnet B).

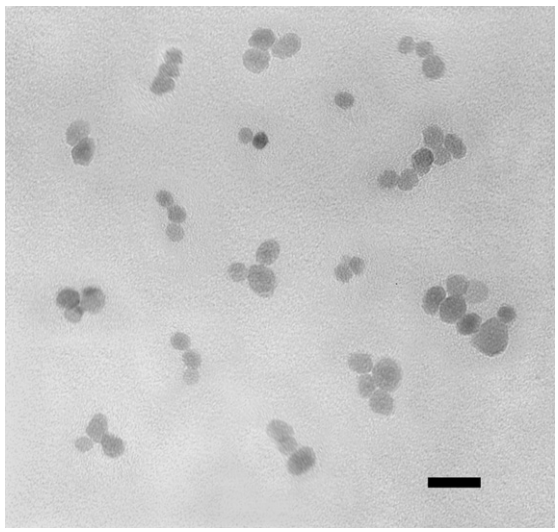

Figure 7. TEM image of starch coated MNP. Bar: 30 nm.

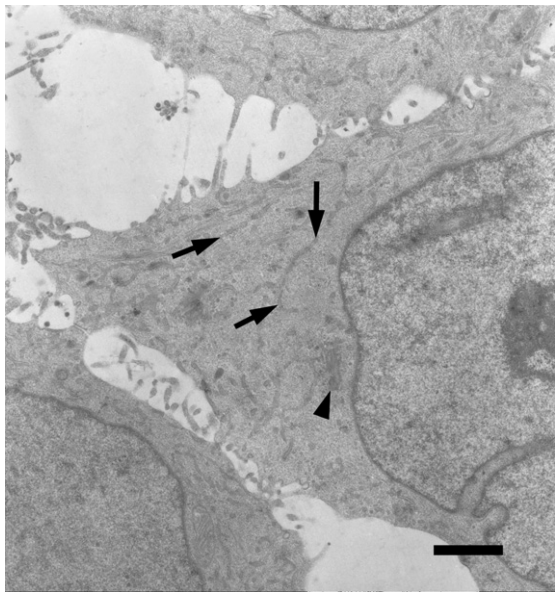

Figure 8. BT-474 cells in culture without exposure to MNP. A regular scattered endoplasmatic reticulum (arrows) and golgi apparatus without any distinct vesiculation was observed (arrowheads). Bar: 1.5 μm.

(e.g. blood perfusion) are influencing factors, the potential temperature elevation in the *in vivo* situation may be reasonably extrapolated [8, 35]. Then, it should become clear whether the temperature range of 55–60 °C for which cytotoxic effects on tumour cells were already reported [14, 36] can be reached with the present approach. The presently found concentrations of Fe were nearly 150 pg/cell, which corresponds to a mean concentration of 0.1 g iron oxide per cm^3 assuming a mean cell diameter of approximately 15 μm. According to previous estimates of the demand for specific heating power for MNP hyperthermia by Hergt *et al* [8], a concentration of 0.01 g cm^{-3} should be sufficient to treat large tumours successfully using MNP. Accordingly, a therapeutically effective temperature elevation *in vivo* would require about 1% of the tumour cells to be labelled with MNP. Nevertheless, whether this concentration can actually be reached by magnetically induced cell labelling *in vivo* has to be clarified.

3.4. Electron microscopical observations

TEM analysis revealed nearly spherical shaped magnetic cores of MNP with a distinct heterogeneity of their diameters (figure 7). The statistical analysis clearly demonstrated a significant normal distribution of measured diameters (data not shown). The mean diameter was 13.36 ± 3.33 nm. Compared with results of VSM (11.4 nm, $\sigma = 0.38$), only a slight difference of calculated mean core diameters could be detected. This observation may be attributed to a better individual consideration of mean variations of diameters of MNP by utilization of TEM analysis.

BT-474 cells in culture without exposure to MNP revealed only a moderately formed endoplasmatic reticulum scattered over the entire cytoplasm. Furthermore only a few golgi stacks without any tendency to vesiculation were detected (figure 8).

Exposing cultivated BT-474 cells to MNP resulted in the distribution of numerous extremely large endosomes over the whole interior of the cell. There was no evidence for the exocytosis of endosomal contents or their release into the cytoplasm. Although the distribution patterns of the MNP in endosomes were not equal in general the integrity of endosomal membranes seemed to be unaffected. Some endosomes revealed a remarkable tendency to merge with primary lysosomes (figures 9, 10). However, in striking contrast to the above-described intracellular processes, after incubating BT-474 cells with MNP, no distinct vesiculations of endoplasmatic reticulum or the golgi apparatus was detected. The present results are in principle concordance with previous investigations by Holzapfel *et al* [37] using MNP encapsulated in polystyrene. However, in the present approach cell cultures

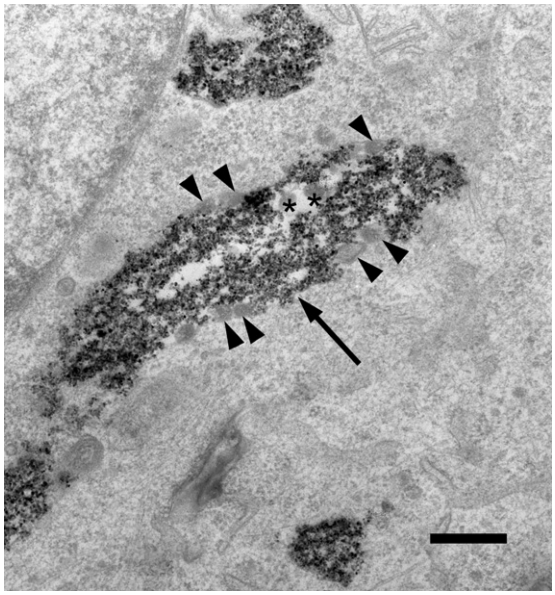

Figure 9. Endosome (arrow) with primary lysosomes in immediate neighbourhood (arrowheads). Asterisks indicate primary lysosomes entered the endosomal interior. Bar: 0.5 μm.

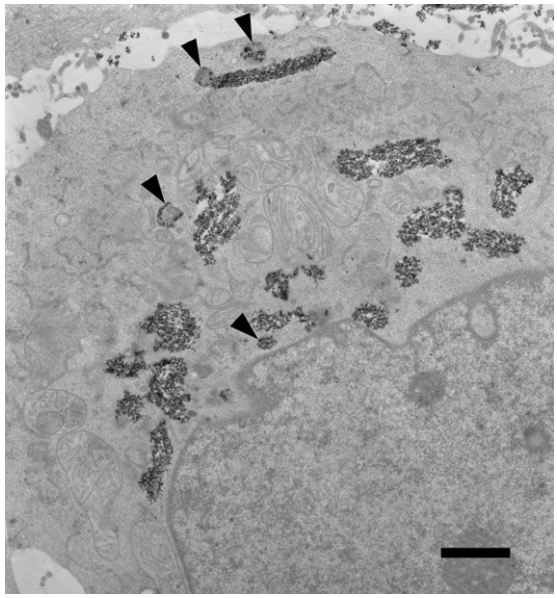

Figure 10. Cultivated BT-474 cells after 24 h exposure to MNP. The cytoplasm is filled with endosomes as well as secondary lysosomes with deposits of MNP (arrowheads). Bar: 1.5 μm.

incubated with starch coated MNP clearly demonstrated a higher efficiency of uptake and accumulation of particles in endosomes. In comparison to other reports [37], amount and size of endosomes also seemed to be significantly higher. Moreover, numerous appearances of primary lysosomes towards endosomal membranes as well as final depositions of MNP in secondary lysosomes were remarkable. However, no uptake in endoplasmatic reticulum, golgi apparatus and mitochondria could be observed. These findings are also supported by former investigations [38, 39]. Otherwise, in direct contrast to previous reports by Lorenz *et al* [38], no binding of MNP to the nuclear envelope could be detected.

It can be summarized that uptake and accumulation of MNP in endosomes as well as their final storage in lysosomes are decisive events of magnetic labelling of cell cultures. It confirms the above described measurements of magnetic induced temperature increases of cells after incubation with MNP.

In the light of the aimed combination with magnetic heating, the present results related to MNP cell labelling suggest that a highly specific concentration of magnetic particles *in vivo* should be possible, as previous investigations on magnetic drug targeting have shown [18–23]. Using magnetic drug targeting, a highly specific concentration of the chemotherapeutic mitoxantron coupled to MNP was achieved *in vivo* within the tumour regions of rabbits [20–22]. Consequently, further improvement of the therapeutic effect should be feasible when this technique is combined with magnetic heating *in vivo*, particularly since hyperthermia is thought to both enhance the effectiveness of chemotherapeutics and diminish drug resistance in cancer cells [40]. In this light, the present results show that MNP may be a versatile tool for combining different therapeutic modalities, namely magnetically induced cell labelling and magnetic heating. These encouraging preliminary results suggest the need for further work dealing with the combination of these methodologies for cancer treatment.

4. Conclusions

Our results showed that it is possible to increase MNP concentration in tumour cells by magnetically induced cell labelling depending on the magnetic field gradient. The intracellular accumulation of MNP is concentrated in endosomes and seems to be ultimately deposited in secondary lysosomes. Higher levels of MNP accumulation resulted in significantly higher temperature increases during magnetic heating treatments in an alternating magnetic field. Consequently, MNP may become valuable tools for combining magnetically based therapy modalities in the future.

Acknowledgments

The present investigation was supported, in part, by the ‘Deutsche Forschungsgemeinschaft’ within the framework of the DFG-priority program ‘Colloidal magnetic liquids’ under contract nos. HI698/5-1 and HE2878/9-2. Furthermore, we thank Professor Dr Alfred Fahr (Department of Pharmaceutical Technology, FSU Jena) for giving us the possibility to determine the hydrodynamic diameter of our MNP with the Zetasizer Nano ZS. The technical assistance of Alida Braunschweig, Silvia Hein, Yvonne Heyne and Brigitte Maron is gratefully acknowledged.

References

[1] van der Zee J 2002 *Ann. Oncol.* **13** 1173–84
[2] Stauffer P R 2005 *Int. J. Hyperthermia* **21** 731–44

[3] Diederich C J 2005 *Int. J. Hyperthermia* **21** 745–53
[4] Gupta A K and Gupta M 2005 *Biomaterials* **26** 3995–4021
[5] Berry C C and Curtis A S 2003 *J. Phys. D: Appl. Phys.* **36** R198–206
[6] Corot C, Robert P, Idee J M and Port M 2006 *Adv. Drug Deliv. Rev.* **58** 1471–504
[7] Hergt R, Andrä W, dÁmbly C G, Hilger I, Kaiser W A, Richter U and Schmidt H G 1998 *IEEE Trans. Magn.* **34** 3745–54
[8] Hergt R and Andrä W 2006 *Magnetism in Medicine—-A Handbook* ed W Andrä and H Nowak (Weinheim: Wiley–VCH)
[9] Gilchrist R K, Shorey W D and Russel M 1957 *Ann. Surg.* **161** 890–6
[10] Ito A, Shinkai M, Honda H and Kobayashi T 2005 *J. Biosci. Bioeng.* **100** 1–11
[11] Hilger I, Andra W, Hergt R, Hiergeist R, Schubert H and Kaiser W A 2001 *Radiology* **218** 570–5
[12] Hilger I, Hiergeist R, Hergt R, Winnefeld K, Schubert H and Kaiser W A 2002 *Invest. Radiol.* **37** 580–6
[13] Jordan A *et al* 2006 *J. Neurooncol.* **78** 7–14
[14] Hilger I, Rapp A, Greulich K O and Kaiser W A 2005 *Radiology* **237** 500–6
[15] Hilger I, Frühauf S, Andrä W, Hiergeist R, Hergt R and Kaiser W A 2001 *Thermol. Int.* **11** 130–6
[16] DeNardo S J, DeNardo G L, Miers L A, Natarajan A, Foreman A R, Gruettner C, Adamson G N and Ivkov R 2005 *Clin. Cancer Res.* **11** 7087s–92s
[17] Hill R P and Hunt J W 1987 *The Basic Science of Oncology* ed J F Tannock and R P Hill (New York: Pergamon) pp 337–57
[18] Lubbe A S, Bergemann C, Brock J and McClure D G 1999 *J. Magn. Magn. Mater.* **194** 149–55
[19] Lubbe A S, Alexiou C and Bergemann C 2001 *J. Surg. Res.* **95** 200–6
[20] Alexiou C, Jurgons R, Schmid R, Hilpert A, Bergemann C, Parak F and Iro H 2005 *J. Magn. Magn. Mater.* **293** 389–93
[21] Alexiou C, Jurgons R, Schmid R, Erhardt W, Parak F, Bergemann C and Iro H 2005 *HNO* **53** 618–22
[22] Alexiou C, Jurgons R, Schmid R J, Bergemann C, Henke J, Erhardt W, Huenges E and Parak F 2003 *J. Drug Target.* **11** 139–49
[23] Lemke A J, Senfft von Pilsach M I, Lubbe A, Bergemann C, Riess H and Felix R 2004 *Eur. Radiol.* **14** 1949–55
[24] Chantrell R W, Popplewell J and Charles S W 1978 *IEEE Trans. Magn.* **14** 975–7
[25] Halbhuber K J, Hulstaert C E, Feuerstein H and Zimmermann N 1994 *Prog. Histochem. Cytochem.* **28** 1–120
[26] Hergt R, Hiergeist R, Zeisberger M, Glöckl G, Weitschies W, Ramirez L P, Hilger I and Kaiser W A 2004 *J. Magn. Magn. Mater.* **280** 358–68
[27] Alexiou C, Schmidt A, Klein R, Hulin P, Bergemann C and Arnold W 2002 *J. Magn. Magn. Mater.* **252** 363–6
[28] Alexiou C, Jurgons R, Schmid R, Kremer M, Bergemann C and Parak F G 2004 *Eur. Arch. Otorhinolaryngol.* **261** 148
[29] Alexiou C, Arnold W, Klein R J, Parak F G, Hulin P, Bergemann C, Erhardt W, Wagenpfeil S and Lubbe A S 2000 *Cancer Res.* **60** 6641–8
[30] Shinkai M and Ito A 2004 *Adv. Biochem. Eng. Biotechnol.* **91** 191–220
[31] Jordan A, Wust P, Scholz R, Tesche B, Fahling H, Mitrovics T, Vogl T, Cervos-Navarro J and Felix R 1996 *Int. J. Hyperthermia* **12** 705–22
[32] Kettering M, Winter J, Zeisberger M, Alexiou C, Bremer-Streck S, Bergemann C, Kaiser W A and Hilger I 2006 *Rofo* **178** 1255–60
[33] Plank C, Schillinger U, Scherer F, Bergemann C, Remy J S, Krotz F, Anton M, Lausier J and Rosenecker J 2003 *Biol. Chem.* **384** 737–47
[34] Kamau S W, Hassa P O, Steitz B, Petri-Fink A, Hofmann H, Hofmann-Amtenbrink M, von Rechenberg B and Hottiger M O 2006 *Nucleic Acids Res.* **34** e40
[35] Kalambur V S, Han B, Hammer B E, Shield T W and Bischof J C 2005 *Nanotechnology* **16** 1221–33
[36] Hilger I *et al* 2004 *Nanotechnology* **15** 1027–32
[37] Holzapfel V, Lorenz M, Weiss C K, Schrezenmeier H, Landfester H and Mailänder V 2006 *J. Phys.: Condens. Matter* **18** S2581–94
[38] Lorenz M R, Holzapfel V, Musyanovych A, Nothelfer K, Walther P, Frank H, Landfester K, Schrezenmeier H and Mailander V 2006 *Biomaterials* **27** 2820–8
[39] Gupta A K and Curtis A S 2004 *J. Mater. Sci. Mater. Med.* **15** 493–6
[40] Schopman E M, Van Bree C, Bakker P J, Kipp J B and Barendsen G W 1996 *Int. J. Hyperthermia* **12** 241–54